Robot Driven Combined Site-specific Maize Seeding and N Fertilization: An Agro-economic Investigation

Muhammad Abdul Munnaf, Yongjing Wang, Abdul Mounem Mouazen*

Department of Environment, Ghent University, Coupure Links 653, 9000 Gent, Belgium

*E-mail of the corresponding author: abdul.mouazen@ugent.be

Abstract

Autonomous agricultural management combats the labor crisis in farming industry and ensures efficient farm operations, whereas variable rate technology has proven to increase resource use efficiency and reduce environmental impacts. This study developed an autonomous robot-driven combined site-specific seeding and N fertilization solution, whose agro-economic and environmental viability was evaluated in maize. A commercial field in Belgium was scanned using a mobile on-line visible and near-infrared reflectance spectroscopy for predicting soil organic carbon (OC), pH, phosphorous (P), potassium (K), magnesium (Mg), and moisture content (MC). The six on-line soil layers were fused to delineate a management zone (MZ) map and derive recommendations for site specific applications. Recommendations for site-specific seeding (SSS) and site-specific nitrogen fertilization (SNF) were implemented with a robotic-based precision seeder and fertilizer sprayer, respectively, coupled to a field robot. Based on the fertility status, each MZ class was sown with one of the seed rates of 70, 80, 90, 100, 110 kSeeds ha^{-1} by seeding densely in the highly fertile MZ and vice versa (i.e., Kings approach). On the fourth day after seeding, variable N rates of 224, 207, 190, 173, 156 l ha^{-1} were applied according to two strategies, namely, Kings (KA – feeding the rich) and Robin Hood (RHA – feeding the poor). Results showed that SSS followed by SNF-RHA improved grain yield (9.96 t ha^{-1}), compared to uniform rate (UR) (9.74 t ha^{-1}) and SNF-KA (9.52 t ha^{-1}) treatments, hence, increased gross margin by 53 € ha^{-1}, compared to UR. SNF-KA consumed lower N and seed inputs than SNF-RHA and UR, while SNF-RHA used slightly more N by 1.5 kg N ha^{-1}, compared to UR. This SNF-RHA was more profitable than the other two treatments. SNF-RHA also resulted in comparable yields across different MZ classes, by recommending complementary N doses, which was not the case for the SNF-KA. In conclusion, autonomous robot-driven combined maize SSS and SNF-RHA solution is proven to be technically feasible, while being profitable and time-efficient, allowing farmers to do multi-tasks simultaneously. Future work should evaluate the proposed integrated technology solution on different crops and a large number of fields to generalise the results achieved to promote practical applications by farmers.

Keywords: Autonomous farming; Variable rate technology; Sensing and modelling; Decision support system; Spatio-temporal soil heterogeneity; Agro-economics

List of abbreviations

ANOVA	Analysis Of Variance
BDB	Soil Service of Belgium
CSSF	Combined Site-Specific Seeding and Fertilization
DGPS	Differential Global Positioning System
ECU	Electronic Control Unit
EU	European Union
GNSS	Global Navigation Satellite System
H	High
K	Potassium
KA	Kings Approach
L	Low
M	Medium
MARS	Mobile Agricultural Robot Swarms
MC	Moisture Content
Mg	Magnesium
MH	Medium-High
ML	Medium Low
MZ	Management Zone
N	Nitrogen
NDVI	Normalised Difference Vegetation Index
OC	Organic Carbon
P	Phosphorus
PTO	Power Take-Off
R^2	Coefficient Of Determination
RHA	Robin Hood Approach
SNF	Site-Specific Nitrogen Fertilization
SSS	Site-Specific Seeding
UR	Uniform Rate
Vis-NIRS	Visible and Near-Infrared Reflectance Spectroscopy
VT	Virtual Terminal

1 Introduction

Seeding and nitrogen (N) fertilization are major farming managements that cover major portions the crop production costs, and the latter strongly affects the soil and water environment (Bünemann et al., 2006; Silva et al., 2013). Traditionally farmers apply both seeds and fertilizer uniformly over the entire field area, assuming no within-field variability exists, despite the fact that most agricultural soils are highly heterogenous both in time and space. Within-field variability necessitates the application of variable rate of inputs, allowing crops to grow optimally over the different zone of a field, protecting

environment, maintaining agro-ecological balances, and increasing the resource use efficiency (De Benedetto et al., 2013; Diacono et al., 2013). Site-specific technologies enable managing within-field variabilities by tailoring the input application rates to match the within-field variations (Munnaf et al., 2020). There are three methods of site-specific applications reported in the literature, namely, map-based, sensor-based, and map-sensor-based (Guerrero et al., 2021a). Map-based application is a MZ oriented method, which divides a field into multiple evenly fertile zones, known as management zone (MZ), based on either one or multiple soil and crop qualitative attributes (Nawar et al., 2017). When a MZ map is available, a unique application rate is assigned to each MZ class according to the fertility status. Assigning the best rate for a specific MZ class is very complex decision that requires accounting for several factors including field history, experts' knowledge, meteorological instances, on top of soil fertility and crop genomics (Munnaf et al., 2020a). However, simple methods for calculating recommendations for map-based technology are mainly based on two methods, namely, the Kings (KA) and Robin Hood approach (RHA) (Munnaf and Mouazen, 2021). The KA recommends a high input rate for the highly fertile MZ and *vice* versa, while RHA follows the opposite principle by recommending low input rate for the most fertile MZ and vice versa. Several studies evaluated the individual effect of either site-specific seeding (SSS) (Munnaf et al., 2021) or site-specific N fertilization (SNF) (Guerrero et al., 2021b), reporting agronomic, economic, and environmentally profits. For example, Munnaf et al. (2022, 2020b) reported that the SSS-KA approach has resulted in profitability for potato (380–597 € ha^{-1}) and maize (93 € ha^{-1}), using MZ maps delineated with fusion of high-resolution data of soil fertility indicators and crop normalized difference vegetation index (NDVI). Another study (Munnaf and Mouazen, 2023) using an on-line visible and near infrared spectroscopy (vis-NIRS) sensor adopted KA method to control seeding rates of fodder maize. They installed an on-line vis-NIRS sensor in front of a tractor to measure a soil fertility index, whose real-time collected values are used to calculate and implement different seeding rates. This was indeed an advanced technical solution of sensor-based SSS, which resulted in increases in yield and gross margin of about 92 € ha^{-1} . Likewise, SNF often increased both yield and gross margin and reduced N input to the environment, despite the RHA outperforming the KA in most cases. Guerrero et al. (2021b) found SNF-RHA in wheat to increase yield by 10.4 % and reduce N inputs by 19.4 %. Similarly, the RHA-based site-specific manure application was also found to reduce N and P applied and increased yield and economic margin (Zhang et al., 2021). Despite most literature reported results for individual implementation of SSS and SNF, one study evaluated the combined application of SSS and SNF in maize (Kazlauskas et al., 2022). Authors calculated recommendations for SSS and SNF based on soil data and crop N uptake, respectively, reporting yield increase, and reduction in N application (Kazlauskas et al.,

2022). However, these authors have neither evaluated a robotic-driven combined solution of SSS and SNF nor the performance of KA and RHA recommendations for variable N rates management.

Examining the literature one can conclude that the KA method is the most appropriate for SSS rates determination, has been established and justified (Munnaf and Mouazen, 2021). But there is still a debate about the best method to calculate recommendations for SNF. Although few studies found KA to be the best method that led to improved yield and reduced N use, many others reported RHA to either increase or maintain yield with increased N use efficiency and reduced N related pollutants (Basso et al., 2011; Schillaci et al., 2021). With such debate, the comparative performance of KA and RHA methods for combined SSS and SNF (CSSF) application remains undocumented.

The agriculture in the European region is highly reliant on the labor availability both from in- and outside EU member countries. Thanks to the recent growth of mechatronic and automation technologies that have accelerated the development of field crop robots. Several research and industry developments have reported the design and application of robots for crop productions to date, which can be grouped mainly into three core categories i.e., mobile platform for in-field navigation, actuation and end-effector techniques, and target detection and operation planning (Yang et al., 2023). For example, Kitić et al. (2022) reported a robot named Agrobot Lala for automatic soil sampling and real-time analysis for nitrate using a predefined MZ, delineated based on the satellite imagery. This robotic-based application ensuring an optimal number of samples while representing within-field variability. A study by Cruz Ulloa et al. (2022) reported the design and testing of a field crop robot integrated with multiple sensors i.e., laser, multispectral, RGB sensors for selective fertilization in green and red cabbage fields. Iqbal et al. (2020) proposed a robot with a light detection and ranging sensor and depth camera to characterise crop phenological traits accurately (96.8 %) with a navigation precision of 1.6–27 cm at indoor and outdoor conditions. Blender et al. (2016) presented a OptiSisor simulation environment for MARS (Mobile Agricultural Robot Swarms) concept in autonomous farming operations, accomplished through integrated coordination among a group of robots. More importantly, Mao et al. (2020) designed and developed an autonomous spraying and fertilization robot to avoid fertilizer waste from surface injection and improve fertilizer use efficiency. Earlier, Amrita et al. (2015) developed an agricultural robot for automatic soil ploughing and seeding based on the AVR At MEGA microcontroller and ultrasonic sensors. Agricultural robots not only present an opportunity to strengthen agri-food production systems by addressing the labor crisis, but also can play significant role in reducing CO_2 emissions (Gonzalez-de-Soto et al., 2015) and soil compaction (King, 2017). Field crop robot has been reported to increase production profitability through mixed cropping practice (Al-Amin et al., 2023), while having variable profitability depending on labor and fuel price, and the time required of supervising the robotic works (Ørum et al., 2023).

While environmental and food safety concerns necessitate agricultural inputs should be managed precisely (Finger et al., 2019), agro-economic and environmental performances of autonomous farming are not explored widely. Despite the rapid growth of robotics technology in the last decade, many of these technologies are only tested in demonstration sites, lacking proof of their performance under real field applications (Ferreira et al., 2023). Therefore, the objective of this study is to develop an autonomous robot-driven CSSF and evaluate its agro-economic and environmental feasibility in maize production. This study hypothesized that different plant populations due to SSS would require variable amounts of N for optimal crop growth and yield. The novelty of this study is related to two points: (i) successive application of SSS and SNF in maize using on-line measured multi-layers soil data fusion, and (ii) investigation of agro-economic and environmental benefits of CSSF technology using a commercially available field crop robot.

2 Materials and methods

2.1 Study field and management zone

This study was conducted in a 5-ha field located at Melle region (50◦59'10.5''N 3◦49'04.1''E), Belgium in May 2022. The field resides under the temperate maritime climate with an annual average temperature ranging between 8 to 14 °C and precipitation varies from 700 to 850 mm. The field has flat terrain with a mild undulation of varying altitude up to 2.5 m. The field has a silt loam texture soil with clay content ranging from 5.7 to 16.1%, and sand content from 9.2 to 42.6%. A crop rotation of potato/sugar beets, wheat/maize with a seasonal cover crop is followed. Maize was grown in the last two cropping seasons, breaking the regular crop rotation for this field.

MZ map is the backbone of a map-based site-specific application. In this study, six soil fertility indicators were measured with an on-line vis-NIRS (305-1700 nm), developed by Mouazen (2006) that was later used by many studies, reporting its technical specifications and successful use cases (Mouazen and Kuang, 2016; Munnaf et al., 2021). During field sensing in 2021, the on-line sensor recorded 5500 geo-referenced spectra, which were pre-processed before used to predict soil pH, OC, P, K, Mg and MC using previously developed partial least squares regression models (Munnaf et al., 2020b). Development of those spectral models involved a series of spectra pre-processing steps, starting with spectral jump correction, which was sequentially followed by edge trimming, moving average filter, standardization (0 to 1), multiple scatter correction or detrending, Savtizky and Golay (S-G) (Savitzky and Golay, 1964) filtering with 1st order derivative and final S-G smoothing. Models were developed using a calibration dataset consisting of 97 samples, these models were validated

using an independent prediction dataset (41 samples). Those spectral models were found accurate (Table 1) enough to implement variable rate applications likewise a previous study conducted at the same field in 2021 (Munnaf et al., 2021). These spectral models satisfied the condition set by Maleki et al. (2008), who suggested a model should achieve the coefficient of determination (R^2) higher than 0.70 to be usable in variable rate application development.

Table 1 Quality of vis-NIRS spectral models used for assessing foil fertility.

Soil fertility attributes	Cross-validation (97 samples)				On-line prediction (41 samples)		
	R^2	RMSE	RPD	LV	R^2	RMSE	RPD
pH	0.76	0.33	2.03	7	0.71	0.36	1.88
OC, %	0.66	0.15	1.73	10	0.65	0.13	1.71
P, mg $100g^{-1}$	0.73	4.88	1.92	9	0.68	4.40	1.78
K, mg $100g^{-1}$	0.64	7.37	1.69	8	0.64	6.08	1.68
Mg, mg $100g^{-1}$	0.80	7.25	2.22	5	0.76	5.96	2.08
MC, %	0.89	1.84	2.98	7	0.87	1.97	2.86

OC, organic carbon; P, phosphorus; K, potassium; Mg, magnesium; MC, moisture content; LV, latent variables; R^2, coefficient of determination; RMSE, root mean square error; RPD, residual prediction deviation.

The on-line predicted six soil attributes were interpolated with semi-variogram (Table 2) analysis followed by ordinary kriging, which predict unknown values of unsampled points by considering the distance as well as autocorrelations between neighboring observations and point of unsampled locations. Soil layers were spatially overlaid and resampled to a 5 m by 5 m grid, using a raster analysis to ensure a spatially homogenous dataset for the cluster analysis to follow. The k-means clustering was employed on spatially homogenous data matrix with a maximum of 100 iterations to develop a MZ, whose number of clusters was decided depending on the minimization of within-cluster sum of squares as a function of the cluster numbers (Daszykowski et al., 2002). MZ was further explored by calculating and visualizing the normalized mean of each property per MZ, followed by ranking MZs into 5 classes of high (H), medium-high (MH), medium (M), medium-low (ML) and low (L) fertile MZ. Both MZ number and the fertility class ranking were cross-verified with the farmer, meaning that MZ delineation considered not only soil data but farmers experience and expert knowledge. Soil mapping and MZ visualization both were accomplished in ArcMap (ESRI ArcGIS™ version 10.7.1, CA, USA), and k-means clustering was analyzed using R in RStudio IDE (RStudio, PBC, Boston, MA).

Table 2 Semi-variogram models used in interpolation of various on-line predicted soil properties by ordinary kriging.

Soil properties	Model	Nugget	Parameter	Range, m	Partial sill	RMSE
pH	Stable	0.091	1.828	15.0	0.082	0.403
OC, %	Stable	0.014	0.678	75.0	0.026	0.209
P, mg $100g^{-1}$	Stable	15.482	0.300	272.0	33.878	6.435
K, mg $100g^{-1}$	Stable	30.670	2.000	10.0	45.374	7.864
Mg, mg $100g^{-1}$	Stable	0	0.300	300.0	29.004	4.903
MC, %	Stable	5.654	1.151	139.0	1.084	2.375

pH; OC, organic carbon; P, phosphorus; K, potassium; Mg, magnesium; MC, moisture content; RMSE, root mean square error. Stable model was originally proposed by Montero et al. (2015).

2.2 System integration

The CSSF system integrated a standard field crop robot, a precision seeder, a precision sprayer with section controls, an ISOBUS interface and a virtual terminal (VT) to enable to combined SSS and SNF systems (Figure *1*). A field robot (Robotti 150D, AGROINTELLI, Denmark) was used, which is an autonomous driving vehicle designed to carry farm implements and to perform multiple tasks autonomously. The current robot has two modules each with two wheels. The left module contains a propulsion engine (75 hp), and the right module contains an additional engine (75 hp) to drive the Power Take-Off (PTO; max 28 hp) and power the implement hydraulically (max 200 bar). The two modules connect to each other through a specially designed central boom. A standard three-point linkage installed on the central boom, to mount the seeder and the spray boom, which must fit within the spacing between two modules. For the SSS system (Figure *1* b), a 3 m (4×75) wide precision maize seeder (Kverneland Optima Rigid e-Drive, The Netherlands) was mounted onto the three-point linkage of the robot. A mechanical accessory was required to increase the top link height to maintain parallelogram facilitating implements lifting and lowering. A VT (TOUCH800, Müller-Elektronik GmbH, Germany) was mounted within a specially made IP68 protected control box. Since the current model of the robot had no active ISOBUS support, an ISOBUS basic vehicle harness with 9-pin connector was installed to establish communication between electronic control unit (ECU) of the seeder machine and the VT. A RS232 serial communication cable was installed to purse RTK-level global navigation satellite system (GNSS) positioning data from the GNSS receiver of the robot (Vector V500 Smart Antena, Hemisphere GNSS, Inc., USA), and to transfer geo-locations information to the VT. The VT was compatible with all ISOBUS machines, meaning that the same VT was possible to use in both the seeding and N fertilization systems. For the fertilization system (Figure *1* c), a standard Beyne sprayer (PA 15-18 m / 600-1.000 l, Beyne NV., Belgium) was customized to a 15 m wide boom with section

control of its six sections. The sprayer equipped with a SPRAYER-controller MIDI 3.0 system with standard configuration (Müller-Elektronik GmbH, Germany). The sprayer had a resolute differential global positioning system (DGPS) of 20–30 cm positioning accuracy (A101 Smart Antena, Hemisphere GNSS, Inc., USA), which was connected with VT through a RS232 serial communication. It came with a 500 l fertilizer container, which was within the design load capacity of the robot. The fertilizer sprayer was mounted onto a three-point linkage and PTO shaft, which powered the pump and thus energized spraying. Hydraulic power allowed boom height adjustment over the crop canopy.

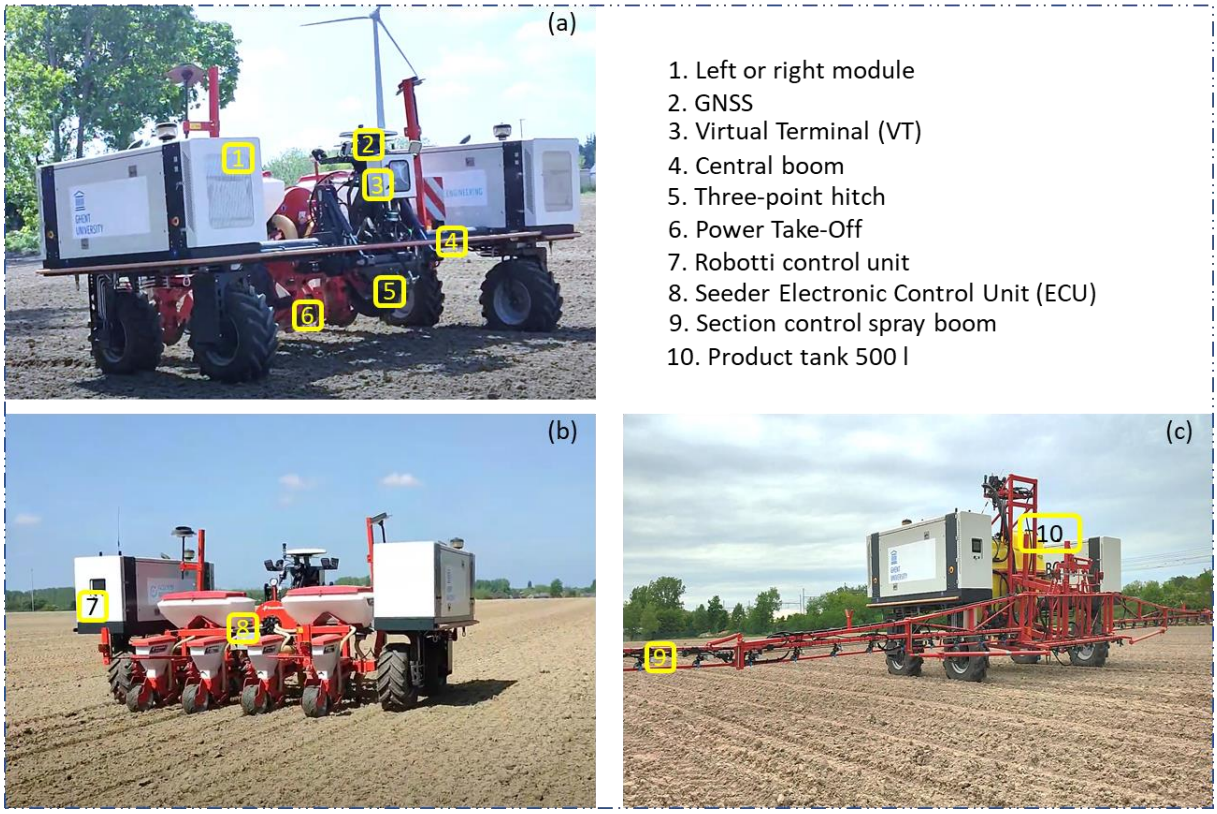

Figure 1: Integration of a maize seeder and a sprayer with a multi-purpose field robot (a) for combined site-specific seeding (b) and nitrogen fertilization (c).

2.3 In-field site-specific applications

Two site-specific applications were implemented back-to-back i.e., seeding followed by N fertilization. Ahead of soil preparation, pig slurry was injected at a rate equivalent of 90 kg N ha^{-1} homogeneously throughout the field. Afterward, the field was ploughed followed by seedbed preparation using the combined tillage machinery having a disc plow, a spiked tooth, and a disc harrow. Based on the MZ map developed in advance relying on soil fertility (Figure *2*), an application task card was prepared for SSS, while seed rates corresponded to the MZ fertility classes were calculated according to the KA principles, and maize was sown. On the 4th day after sowing, variable N fertilization rates were sprayed using a second task card prepared, which allowed comparison between KA and RHA principles with

the traditional UR treatment. This was done using a parallel strip (Figure 3) overlaid the MZ map, whose details will be explained below.

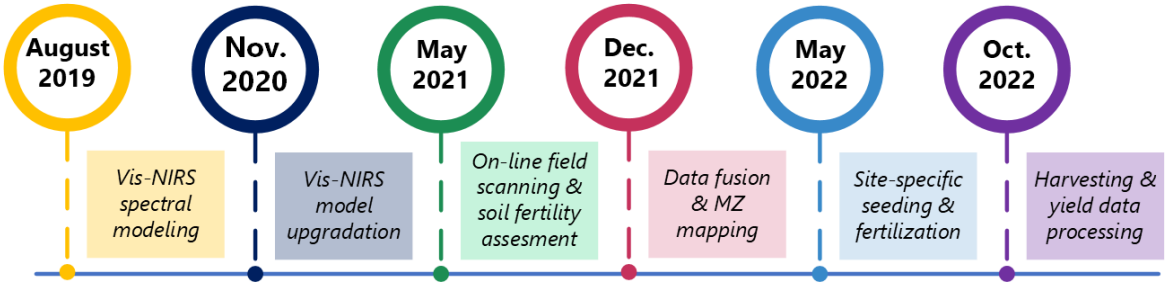

Figure 2: Timeline chart of various steps, encompassing the spectral modeling, field scanning, management zone (MZ) delineation, site-specific seeding and nitrogen fertilization, and yield data processing phases.

2.3.1 Route planning

Route planning of the robot was developed and configured several machine and operational parameters through the official cloud platform (Robotti 150D, AGROINTELLI, Denmark). It started with uploading field boundary as geodata format (.shp) followed by implement configuration. The working width of the seeder machine and the sprayer were set to 3 m and 15 m, respectively. Working length was set to equal the field length, whereas working speed was set to 4 km hr^{-1}. The PTO speed was set to 540 rpm, while the three-point-linkage height was set to 45 cm and 75 cm for the seeder and sprayer, respectively. In both cases, headlines mode of operation was chosen to ensure 15 m boundary area to manage through a separate path plan to avoid any misalignment of the experimental treatments and border zone. Finally, the route plan was transferred from the cloud server to the robot to start operations and was downloaded to guide in designing of application maps.

2.3.2 Site-specific seeding

A parallel strip experiment was designed, which overlaid the MZ map. The path lines of the robot were specified to ensure the robot passing through the strips in a way to ensure the right placement of desired application rates. Strips were 30 m and 15 m wide for SSS and homogenous seeding treatments respectively. The strips of former treatment were divided into sub-strips (plots), depending on the size of MZ class underneath. Afterward, a unique seed rate was assigned to each of the plots. Being inspired from a previous study (Munnaf and Mouazen, 2021), SSS rates were determined according to the KA approach (feeding the rich), i.e., recommending the highest seeding rate for the most fertile MZ, and vice versa. Seeding rates of 70, 80, 100 and 110 kSeeds ha^{-1} (1000 seeds ha^{-1}) were recommended for L, ML, MH, and H fertile MZ classes, respectively, while 90 kSeeds ha^{-1} was decided for the control UR seeding treatment. Geo-referenced application map (i.e., task card) was created by using ArcMap (ESRI ArcGIS™ version 10.7.1, CA, USA) and exported as machine-

compatible shapefiles with a geographic coordinate system of WGS 1984 (Figure 3). The maize hybrid, Milkmax was sown on 6th of May 2022.

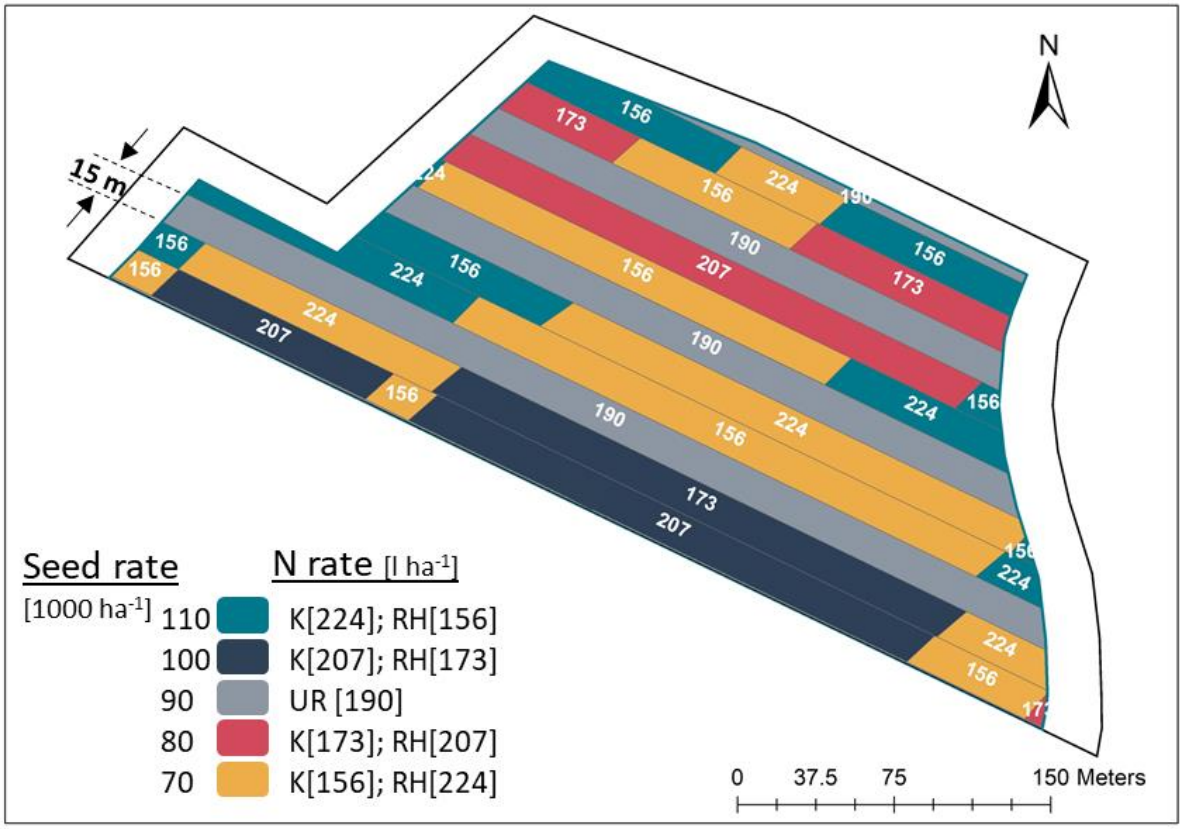

Figure 3: Application map of combined site-specific seeding and two site-specific nitrogen (N) fertilization treatments i.e., Kings approach (KA) and Robin Hood approach (RHA), compared with uniform rate (UR) treatments of seeding and N fertilization.

2.3.3 Site-specific N fertilization

Each of the 30 m wide strips of the SSS treatment was longitudinally split into two strips of 15 m each, meaning that plots of both splits were seeded with the same seed rate. One of each paired strips received one SNF with two different N doses recommended by KA and RHA strategies. This led to generate a total of three groups of strips (each having 15 m width) to allow three treatments i.e., SNF-KA (site-specific N fertilization recommended by KA), SNF-RHA (site-specific N fertilization recommended by RHA), and UR treatment (uniform N over homogenous seeding). The RHA follows the opposite principle of KA, by recommending the highest N dose for the poorest fertile MZ, and vice versa. Since the field was initially fertilized with 90 kg N ha^{-1} by injecting pig slurry, only the remaining portion (75 kg N ha^{-1}) of the recommended N dose (165 kg N ha^{-1}) was implemented in this experiment. Accordingly, a rate of 75 kg N ha^{-1} was designated for the UR treatment, and rates of N in the SNF treatment varied over 61, 67, 81, 87 kg N ha^{-1} for L, ML, MH, H fertile MZ, respectively, in SNF-KA, and

for H, MH, ML, and L fertile MZ respectively in SNF-RHA treatments. A commercial liquid N product (specific weight = 1.3 kg l^{-1}) containing 30 % N was sprayed in this study, leading the corresponding application rates to 224, 207, 190, 173, 156 l ha^{-1}. Likewise seeding, a geo-referenced application map (Figure 3) was created and used for spraying N fertilizer on 10th of May in 2022, before seed germination.

2.4 Crop management and harvesting

Crops were grown under rainfed conditions, and there was no foliar fertilization after seed germination. Herbicide was sprayed at 3–4 leaf stage to control weed infestation only once. Influences of other management operations i.e., tillage, herbicide, and weather conditions on crop growth were homogenous across SSS and SNF treatments evaluated in this study. On the 22nd of October 2022, grain was harvested using a combine harvester (New Holland CX7.90, New Holland, USA) equipped with a yield monitoring system. It estimated grain yield by measuring grain mass-flow (throughput) per second with an average travel speed of 7 km hr^{-1} with geo-referencing by a GNSS.

2.5 Harvest and economic analysis

Geo-referenced yield data were first filtered to remove erroneous coordinates, outlier observations, missing values and so on. Yield measured at the border strip of 15 m wide around the field was discarded to avoid any possible border influences on the measured yield. Observed yields were projected over the application map to join spatially (i.e., synchronizing observed yield points with application locations), and each strip provided an average yield corresponding to treatments. An average yield of each treatment was used for the cost-benefit analysis using the partial budgeting approach (Roth, 2017). The partial budget focused only on changes in income and expenses that would result from implementing a specific alternative strategy. Thus, all aspects of farm profits that were unchanged by the decision can be safely ignored. The revenue, product of maize grain yield (t ha^{-1}) and market price (250 € t^{-1}), was considered as the production outcome while the seed cost (225 € ha^{-1} @ seed rate of 90 kSeeds ha^{-1}) was counted as the input production cost. Apart from calculating the gross margin per treatment, simulated gross margin per field was estimated as if one treatment was applied throughout the entire field area. Additionally, the total amount of fertilizer applied was compared among the treatments, and simulations of fertilizer use and savings per treatment were also calculated. Note that all other costs such as soil analysis, sensing, land preparation, herbicide, harvesting, and operational costs were assumed to be consistent for all treatments.

2.6 Statistical analyses

The quality of MZ map developed with K-means clustering was evaluated using Silhouette statistics (Rousseeuw, 1987) through minimization of within-clusters sum of squares. Silhouette score ranges between -1 to +1, with high values indicating perfect separation of the groups whereas lower score indicates clusters may have overlapping observations that can be assigned to another cluster. One-way analysis of variances (ANOVA) was conducted on the observed grain yields to evaluate whether mean yield of the proposed treatments was significantly different from each other. The yield responses to the variable seed and N rates were assessed through polynomial curve fitting, and goodness of fit was evaluated using R^2 statistics. Key soil fertility attributes affecting grain yields were identified through Pearson's pairwise correlation analysis carried out among on-line predicted soil attributes and yields observed per treatment.

3 Results and discussion

3.1 Within-field spatial heterogeneity

On-line map of each soil property illustrates large within-field variability with different extent of spatial structures (Figure 4). Accordingly, the k-means clustering algorithm identifies MZ classes (i.e., H, MH, ML and L) through minimization of the within-clusters sum of squares against the cluster numbers. MZ clustering scores a bit lower Silhouette width (0.23) than that was observed in a previous study worked with a similar dataset (Javadi et al., 2022), indicating that many of the observations can be distributed between two clusters and these carry identical characteristics at least to some degrees. Use of 5 m by 5 m rasterized matrix in MZ delineation generates an enormous number of observations, which are likely to have some similarity among the observations and may explain the poor Silhouette width in MZ clustering. Normalized mean plot (Figure 4 b) indicates a confusing contribution of each soil property to MZ clustering and ranking, suggesting to provide different weights to each of the different soil attributes. Cluster 1 referring to the H fertile MZ mainly has the highest amount of available P and Mg along with the second highest pH, K and MC. The MH fertile zone (cluster 4) embodies the highest pH and OC, the second highest P with the least amount of MC, and Mg contents. The ML fertile MZ (cluster 2) has the lowest concentration of OC, although it has the highest K and MC and the second highest Mg, while the least fertile (L) MZ (cluster 3) contains mostly the least amount of half (e.g., K, pH and Mg) of fertility indicators.

Between MZ clusters variation in soil K concentration reveals two different K intensity zones, with the cluster 2 (ML fertile MZ) can be considered as the K-rich zone, while rest of the MZ clusters having poor K with almost equal K concentrations. The observable agreement between soil pH and P spatial

distributions confirms the regulatory impact of pH on soil P availability (Hopkins, 2013). Optimal pH for sufficient P availability can vary according to soil texture types (Van Vliet and Giller, 2017), however, the current field having a silt loam texture is likely to ensure abundant amount of P availability at a pH around 6.37–7.53. Opposite spatial distribution pattern between pH and OC, for the top half of the field, can be attributed to the rapid decomposition of organic matter leading to increase organic acids production and thus reduce soil pH level (Zhou et al., 2019). Spatial similarity between K-rich and high MC area reveals the large K's movement to the plant roots and enhanced K availability (Naumann et al., 2020). Least concentration of Mg along the bottom edge of the field can be attributed to the fact that phosphate ions (PO_4^{-3}) reacting with Mg to form less soluble compounds, and thus making Mg less available (Lu et al., 2022), which is further influenced by low MC availability in the same area. Worth noting that all MZ classes, however, satisfies the required fertility levels recommended by BDB (Soil Service of Belgium) for optimal crop growth (pH = 6.5–7.0; OC = 1.2–1.6%; P = 13–21, K = 15–23 and Mg = 9-16 in mg 100 g^{-1}). Variable soil fertility among MZ classes explains the necessity for site-specific management, which is evaluated in this study for the combination of seeding and N fertilization.

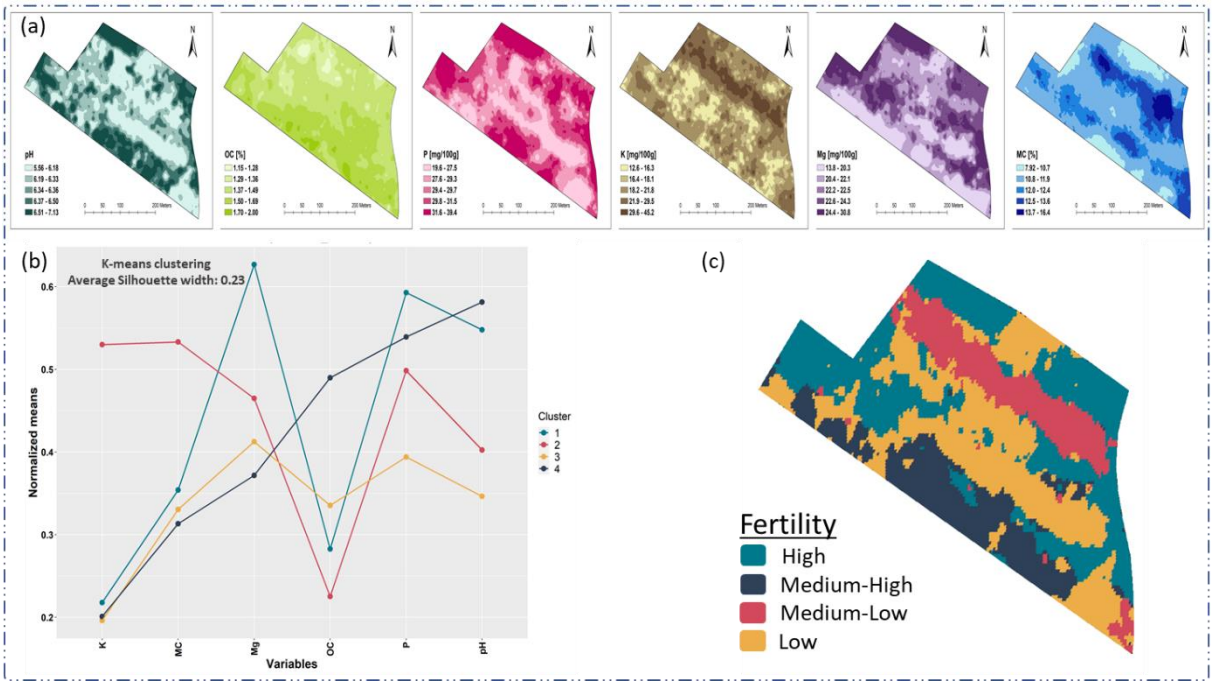

Figure 4: On-line predicted soil maps after ordinary kriging (a), normalized mean of variables in each cluster after k-means cluster analysis (b), and management zone map with fertility ranks (c).

3.2 Yields response to variable rates

Yield response to N doses follows a typical production function i.e., yield increases with increasing N inputs until reaching a peak followed by a gradual declination (Figure 5). Despite good second order

polynomials between yield and N applied in MZ for both SNF-KA and SNF-RHA treatments, different yield-to-N response is observed. Highly fertile MZ-H when fertilized with 156 l ha^{-1} produces higher yield in RHA than that is observed in KA for the MZ-L receiving the same N rate. RHA increases yield at the MZ-L with the highest N application rate (224 l ha^{-1}) whereas KA results in a yield reduction in the MZ-H in receipt of the N same dose. Both KA and RHA agree on an agronomic optimal N rate of around 190 l ha^{-1}, which was equal to the UR treatment.

Between-treatments differential yield-to-N responses can be attributed to the different fertility status of MZ classes that should support different plant densities and supply required amount of nutrients including N to the crop. RHA approach improves grain yield in L, ML, and H fertile MZ classes compared to corresponding yields observed in KA treatment. This indicates that the highly fertile MZ-H does not require a high N rate (as recommended by KA) to produce the highest yield, and that the poorly fertile MZ-L requires a high N dose to maximize yield. Ideally, RHA should equalize yield across different MZ classes by suggesting N doses complementary to the fertility of each MZ class. However, the current SNF-RHA cannot perfectly equalize yields across MZ classes because MZs have been sown with different seed rates, which may already neutralize the potential influence of within-field fertility variations on yields, and thus questioning the need for successive SNF practice. This is apparently observable in yield to seed rates quadratic response curve (Figure 5 b), showing that seed rates higher and lower than the rate of around 190 l ha^{-1} has reduced crop yields. Low seed rates have yielded quite higher in L and ML fertile MZ in the SNF-RHA treatment, because of higher N inputs applied than those applied in the SNF-KA treatment. Contrary, high seed rates in MH and H reveals similar yielding pattern with smaller differences between the SNF treatments than for ML and L, indicating yield of fertile MZs (both H and MH) is less sensitive to variable N rates. Therefore, extra N rate than necessary in H and MH, as the case of SNF-KA will have a negative agronomic and environmental effects by increasing N leaching potential.

One way to maximize output by site-specific applications is to produce similar yield at different zones while receiving the optimal rates of input in each zone. This was not the case in the current work, by the combined use of SSS and SNF, particularly for the SNF-KA (Figure *5*). The small success in yield equalization observed for the SNF-RH is probably due to fact the percent changing of seed rates across different zones were decided arbitrarily. This iterates a question to answer in future work, whether a site-specifically seeded field would need to be fertilized with variable N rates, if so a second question would be how to optimize N rate per MZ receiving variable seed rates. Perhaps, a series of plot experiments should account for all combinations of seed and N rates under specific controlled conditions will enable answering these two questions. From the current study, it is difficult to explain further the reasons for yield variability whether it is due to variable rate seeding or N fertilization

rates. However, the individual practice of SSS in maize (2.0–4.4 %) (Munnaf et al., 2022) and potato (2.6–13.4 %) (Munnaf et al., 2021), as well as SNF in wheat (1.5 %) (Zhang et al., 2021) and barley (11.6 %) (Guerrero et al., 2021b) has been reported to increase yields repeatedly. A recent study has also found that SSS followed by SNF to increase yield (by about 5.5 %) and yield contributory components (e.g., ear density, kernels per ear) and to save N inputs by 14 kg N ha^{-1} (Kazlauskas et al., 2022). Unlike the current study, their study calculated N doses according to crop N uptake measured by a Yara crop N sensor instead of taking seeding rates and MZ soil fertility into consideration.

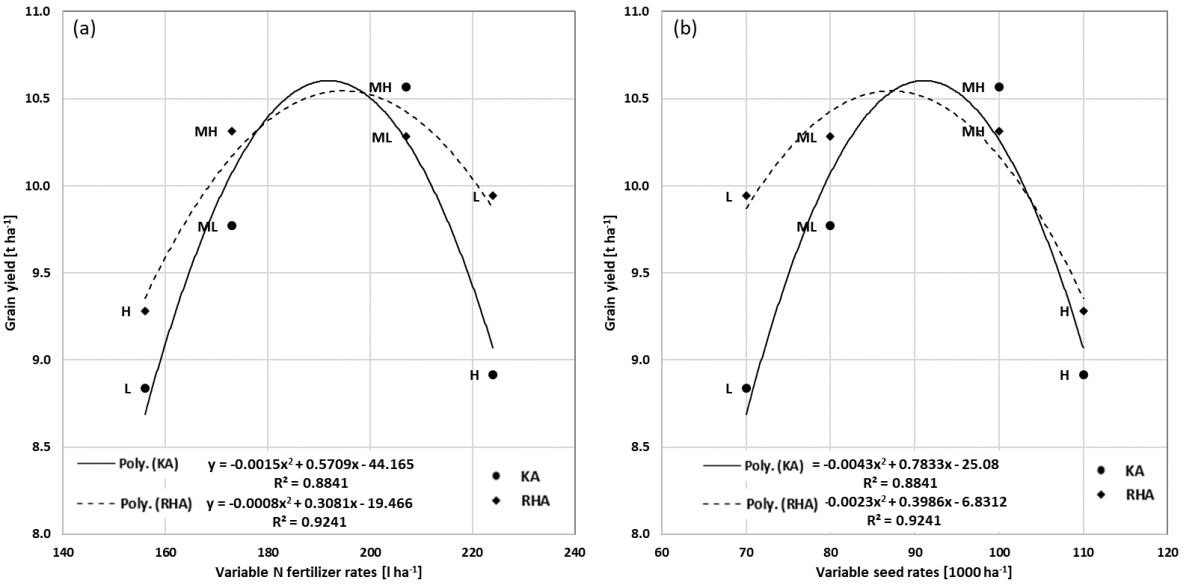

Figure 5 Response of maize grain yield to variable nitrogen (a) and seeding (b) rates recommended by Kings (KA) and Robin Hood (RHA) approaches for high (H), medium-high (MH), medium-low (MH) and low (L) fertile management zone.

3.3 Productivity and profitability analysis

SNF-RHA increases grain yield compared to the UR as well as SNF-KA treatments with an increased gross production margin (Table 3). Both SNF treatments have consumed lower average seed density (KA: 84.83 and RHA: 87.74 kSeeds ha^{-1}) than the UR application (90 kSeeds ha^{-1}), indicating a low soil fertility that is unlike to support 90 kSeeds ha^{-1}. A similar seed rate of 86.5 kSeeds ha^{-1} was reported for this field in a previous study evaluating a sensor-based SSS application (Munnaf and Mouazen, 2023). For the SNF-KA treatment, average N consumption is reduced by 3.43 kg ha^{-1}, while in the SNF-RHA treatment slightly more N (1.5 kg ha^{-1}) is used than the UR treatment. The yield of SNF-RHA treatment is higher (9.96 t ha^{-1}) than UR (9.76 t ha^{-1}) treatment, and much higher than SNF-KA (9.52 t ha^{-1}). Yield improvement is, however, not statistically significant (p=0.39) at a 95 % level of confidence (Table 4), and thus one can hardly expect a similar outcome by implementing the proposed CSSF technology in this same field. However, compared to the UR treatment, the SNF-RHA treatment has

resulted in an increased gross margin by 54 € ha^{-1}, which can be simulated as high as 231 € ha^{-1} if the entire field was possible to be managed using SNF-RHA method. It is worth noting that the profitability of CSSF applications mainly emerges from the increased grain yield rather than inputs saving, which is in line with results reported in earlier studies for SSS (Munnaf et al., 2020a, 2020b). Examining further the economic returns on N costs reported in the literature, one may come to similar conclusions to the current findings. For example, an earlier work reported a net return of 15.2–24.64 € ha^{-1} from SNF in maize, compared to the traditional UR fertilization practice (Koch et al., 2004). Stamatiadis et al. (2018) reported a sensor-based SNF to increase revenue over N costs by 118 € ha^{-1} without a yield reduction. Both Stamatiadis et al. (2020) and Evangelou et al. (2020) reported sensor-based SNF in maize to increase returns on N costs of about 33–92 € ha^{-1}. Compared to UR N fertilization, Guerrero et al., (2021b) reported an increased gross margin of 129.27–148.78 € ha^{-1} and 4.85–16.40 € ha^{-1} in two fields with barley and wheat, respectively. Zhang et al. (2022, 2021) observed an increase in gross margin of 36.32 and 40.06 € ha^{-1} by variable rate manure using the RHA, and KA, respectively, using a MZ map delineated by data fusion of on-line collected soil fertility attributes (like the soil data in current study) and crop NDVI. Recently Munnaf et al. (2023) reported SNF to increase gross margin by 43.93 € ha^{-1} in winter wheat by implementing a novel map-sensor-based solution.

Assuming the cost of the on-line soil sensing of 25 € ha^{-1}, and that the labor saving of 70 € hr^{-1} (based on local labor market) can be made by the robot-based site specific implementation, under an environment where the purchase cost of a robot would be equivalent to that of a tractor, a net return of 99 € ha^{-1} (54 € ha^{-1} [gross margin] – 25 € ha^{-1} [cost of soil scanning] + 70 € ha^{-1} [saving on labor by robot]) can be made. Nonetheless, the current analysis excluded saving on labor to run the robot, given the fact that an operator had to monitor the system for safety requirement and local legal issues (article 59/1, Ministry of Mobility, Belgium). Assuming there were no such legal requirements or if one operator could oversee multiple units simultaneously, operating costs could be likely reduced significantly, increasing profitability beyond what this study calculated of 54 € ha^{-1}, compared to the traditional UR application. However, with the Green Deal by the European Commission, SNF should focus more on N input reduction than yield increase as suggested in earlier studies (Ehlert et al., 2004; Stamatiadis et al., 2018). These studies found that SNF increases or maintains the same yields. In the current work, profitability stems from the increase in yield of the SNF-RHA treatment, over both the UR and SNF-RH treatment, while using slightly more N of 1.5 kg ha^{-1}, compared to UR (Table 3).

Table 3 Partial budgeting-based cost-benefit and inputs use analyses for the combined site-specific seeding and nitrogen fertilization (CSSF) in maize.

Account items	**Treatments**								
Methods	**UR**	**KA**				**RHA**			
Management zone	**-**	**H**	**MH**	**ML**	**L**	**H**	**MH**	**ML**	**L**

Area, ha	1.25	0.23	0.41	0.18	0.75	0.36	0.29	0.29	0.52
Fertilizer rate, l ha^{-1}	190	224	207	173	156	156	173	207	224
Total fertilizer applied l $plot^{-1}$	238.06	51.42	84.27	31.30	116.58	56.28	49.95	60.72	117.48
Average N use, kg ha^{-1}	74.10	70.67				75.60			
Relative N use, kg ha^{-1}	-	**-3.43**				**+1.50**			
Simulated relative N use, kg ha^{-1}	-	-14.69				+6.43			
Cost of N, € ha^{-1}	**46.31**	**44.17**				**47.25**			
Seeding rate, 1000 ha^{-1}	90	110	100	80	70	110	100	80	70
Total seeds applied, 1000 $plot^{-1}$	112.76	25.25	40.71	14.47	52.31	39.68	28.87	23.47	36.71
Average seed use, 1000 ha^{-1}	90	84.83				87.74			
Relative seed use, 1000 ha^{-1}	-	**5.17**				**2.26**			
Simulated relative seed use, 1000 ha^{-1}	-	22.16				9.70			
Cost of seed, € ha^{-1}	**225**	**212.07**				**219.34**			
Total seed and N costs, € ha^{-1}	271.31	256.24				266.59			
Grain yield, t ha^{-1}	9.76	8.92	10.57	9.77	8.84	9.28	10.31	10.28	9.94
Average grain yield, t ha^{-1}	**9.76**	**9.52**				**9.96**			
Grain revenue, € ha^{-1}	2440	2381				2489			
Gross margin, € ha^{-1}	**2168**	**2125**				**2222**			
Relative gross margin, € ha^{-1}	-	**–43**				**+54**			
Simulated relative gross margin, €	-	**–187**				**+231**			

UR, uniform rate; SNF-KA and SNF-RHA, site-specific nitrogen fertilization through Kings and Robin Hood approaches, respectively; H, MH, ML and L, high, medium-high, medium-low, and low fertility management zone (MZ) classes respectively. Some key findings are highlighted as bold texts.

Table 4 Single factor analysis of variance in maize grain yield from combined site-specific seeding and nitrogen fertilization treatments of UR, SNF-KA and SNF-RHA.

Source of variation	**SS**	**df**	**MS**	**F**	**P-value**	**F crit**
Between Groups	1.06	2	0.53	1.04	0.39	4.26
Within Groups	4.56	9	0.51			
Total	5.61	11				

SS, some of squares; df, degree of freedom; MS, mean squares. UR, uniform rate; SNF-KA and SNF-RHA, site-specific nitrogen fertilization through Kings and Robin Hood approaches, respectively.

3.4 Yield association with MZ attributes

Correlations between Maize grain yields and MZ soil attributes differ among the two SNF treatments (Figure 6). A strong Pearson correlation (r = 0.97) between OC and yield in KA indicates the basic function of soil OC to ensure foods for soil micro-organisms and thus increasing microbial community and activity, and soil fertility at large. Increased OC is likely to increase soil water storage and thus water availability to plants and improve nutrient cycling (Bünemann et al., 2018). The more the OC content, more the soils' ability to support high plant density leading to increase crop biomass production and yield in turn (Virk et al., 2020). A poor positive correlation between yield and pH (r = 0.31) explains that yield in the SNF-KA treatment should not vary strongly with pH, despite the reported role of soil pH to regulate P availability with strong positive correlation (Hopkins, 2013).

Although pH should have a negative relation with OC because higher OC content decomposition produces higher organic acids that should reduce soil pH (Zhou et al., 2019), this has not been observed for the SNF-KA treatment. This can be attributed to the small variation of pH across different MZ classes (H = 6.42, MH = 6.47, ML = 6.2 and L = 6.10), which all are considered ideal for crop growth in a silt-loam texture field according to the BDB.

The poor positive correlation between yield and OC (r = 0.34) in the SNF-RHA treatment is partially compensated for by applying high N doses in poorly fertile MZ classes where low OC is observed (Figure *4*). A poor correlation between yield and MC of 0.31 can be observed for the SNF-RHA, is in-line with the similar correlation with OC. Indeed, soil OC and MC work hand in hand in supporting crop development by enhancing water and nutrient availability. The K^+ cation is positively correlated with yield (0.41), indicating its role in plant cell divisions and energy transports from root to leaf (Koch et al., 2020; Naumann et al., 2020). The above discussion suggests that it would be more valuable to only consider soil OC, pH, and MC in future works for the delineation of MZ for variable rate application development. However, it is worth noting that none of the correlations was found statistically significant at 95% confidence interval.

RHA / KA	pH	OC	P	K	Mg	MC	Yield
pH		**0.53**	**0.87**	-0.36	0.23	-0.40	-0.20
OC	**0.53**		0.05	-0.66	-0.60	-0.74	0.34
P	**0.87**	0.05		-0.01	**0.60**	0.00	-0.39
K	-0.36	-0.66	-0.01		0.03	**0.99**	**0.41**
Mg	0.23	-0.60	**0.60**	0.03		0.13	-0.88
MC	-0.40	-0.74	0.00	**0.99**	0.13		0.30
Yield	0.31	**0.97**	-0.20	-0.60	-0.76	-0.69	

Figure 6 Pearson correlations among on-line predicted soil organic carbon (OC), pH, phosphorus (P), potassium (K), magnesium (Mg), moisture content (MC) and yield, harvested from the combined site-specific seeding (SSS) and site-specific nitrogen fertilization (SNF) using the Kings (KA) and Robin Hood (RHA) prescriptions. Bold values stand for correlations higher than 0.40.

3.5 Robot adoption future

Despite the field robot of the current work enabled implementing CSSF (SSS and SNF) successfully in a maize field, several technical issues were diagnosed yet to be solved prior to commercial applications replacing the current tractor-based system. Transporting the robot from farm to field is one of the big challenges, which is highly time consuming and expensive assuming local transportation facility is available. While robots are made for autonomous farm operations, the robot itself cannot or is not legally allowed to walk on the road on its way to the field. This being a multi-purpose field robot, it should allow fitting a few of the most common farm machines. In the current research, only two machines i.e., seeder and sprayer were used, for which several limitations have been identified: (i) low load carrying capacity limits the machine size, (ii) insufficient implement lifting height, (iii) hard to fit machine between two modules of the robot, and (iv) three-point linkage affects parallelogram of implement lifting. The bottom links of the three-point hitch are not adjustable and thus require unnecessary efforts and time to mount the machine, and mounting becomes hard to difficult when the ground surface is not perfectly even, which is always the case at field conditions. The PTO speed cannot be increased gradually, and rotation starts at its maximum set speed, thus endangers seeder vacuum and sprayer pump. Inactive ISOBUS limits applicability to support all sorts of farm machines supporting variable rate technologies, which is the reason why this study had to create an external ISOBUS station, increasing costs and efforts. The current design and the limited traction power of the robot does not allow the simultaneous mounting of the on-line soil sensor and the seeding machine together. In the future, a more powerful robot is necessary to join both for sensor-based SSS, which has great potential to measure soil fertility in a continuous stream of information and can simultaneously control the variable application rates in one run (Munnaf and Mouazen, 2023), resulting in significant time and energy savings.

During the field operation, traction failure at loose soil conditions was observed, hence, a future model should come up with a solution to overcome this important issue. Loose soil together with windy conditions can be very dusty particularly during seeding, often stopping the robot because it affects LIDAR sensor to detect object at the front. Stopping requires a restart of the system, and restarting often sends robot back to the initial starting point to continue working though it can resume tasks but frequently found unresponsive. Time necessary for restarting leads the VT of seeder and sprayer to sleep and thus fails to reinitiate spraying and seeding, which is hard to diagnose immediately. The robot can stop and go off route due to the poor network connection, which is often the case at remote field locations. Based on the above limitations associated with the practical use of the field robot of the current study, further development should be improved to spark farmers interest in adopting robotics for site-specific management of farming input resources.

4 Conclusions

Robot-based combined site-specific seeding (SSS) and site-specific N fertilization (SNF) (CSSF) were implemented and evaluated in maize at a commercial field. Results showed that SSS followed by SNF using Robin Hood (RHA) prescription improved grain yield (by 0.2 t ha^{-1}) and gross margin (54 € ha^{-1}) but consumed a slightly higher amount of N (1.5 kg ha^{-1}) than uniform rate (UR) application, however, yield increase was not statistically significant. Profitability would likely be 231 € if SNF-RHA technology is implemented throughout the entire field.

Results showed SNF-RHA to lead to a smaller variability in yield across different MZs, compared to SNF-KA. However, crop response in terms of yield to high N input rates in fertile MZ seeded densely was poor (as in KA), which can increase N leaching potentials. Future work should establish the best combination of seeding and N fertilization rates for MZs having different fertility levels, which ensure the maximum yield and minimum environmental footprint, e.g., minimum N leaching.

CSSF in maize field was technically possible to implement using an autonomous robot coupled with existing farm machines of a precision seeder and a liquid fertilizer sprayer. For adoption by farmers, there is long trajectory to follow to overcome major limitations associated with the robot transportation from farm to field, low load carrying capacity, inactive ISOBUS support, inflexible three-point linkage to adopt, limited traction, poor network connections, a few to mention among others. The proposed autonomous CSSF is technically sound and agro-economically profitable. Extensive evaluations of full-budget economic analyses examining returns on investment, break-even point, and life cycle assessment are suggested prior to the CSSF adoption at large-scale application. Future studies should expand such investigations to a larger number of fields under different weather conditions using different crops to validate further the result obtained in the current study.

Acknowledgment

Authors acknowledge the financial support received from the Research Foundation - Flanders (FWO) for Odysseus I SiTeMan Project (Nr. G0F9216 N).

References

Al-Amin, A.K.M.A., Dickin, E., Monaghan, J.M., Franklin, K., Lowenberg-DeBoer, J., 2023. Economics of autonomous machines for regenerative agriculture, in: Precision Agriculture ’23. Wageningen Academic Publishers, The Netherlands, pp. 749–755. https://doi.org/10.3920/978-90-8686-947-3_94

Amrita, S.A., Abirami, E., Ankita, A., Praveena, R., Srimeena, R., 2015. Agricultural Robot for automatic ploughing and seeding, in: IEEE Technological Innovation in ICT for Agriculture and Rural Development (TIAR). IEEE, pp. 17–23. https://doi.org/10.1109/TIAR.2015.7358525

539 Basso, B., Ritchie, J.T., Cammarano, D., Sartori, L., 2011. A strategic and tactical management
540 approach to select optimal N fertilizer rates for wheat in a spatially variable field. European
541 Journal of Agronomy 35, 215–222. https://doi.org/10.1016/j.eja.2011.06.004

542 Blender, T., Buchner, T., Fernandez, B., Pichlmaier, B., Schlegel, C., 2016. Managing a Mobile
543 Agricultural Robot Swarm for a seeding task, in: 42nd Annual Conference of the IEEE Industrial
544 Electronics Society. IEEE, pp. 6879–6886. https://doi.org/10.1109/IECON.2016.7793638

545 Bünemann, E.K., Bongiorno, G., Bai, Z., Creamer, R.E., De Deyn, G., de Goede, R., Fleskens, L.,
546 Geissen, V., Kuyper, T.W., Mäder, P., Pulleman, M., Sukkel, W., van Groenigen, J.W., Brussaard,
547 L., 2018. Soil quality – A critical review. Soil Biol Biochem 120, 105–125.
548 https://doi.org/10.1016/j.soilbio.2018.01.030

549 Bünemann, E.K., Schwenke, G.D., Van Zwieten, L., 2006. Impact of agricultural inputs on soil
550 organisms - A review. Australian Journal of Soil Research 44, 379–406.
551 https://doi.org/10.1071/SR05125

552 Cruz Ulloa, C., Krus, A., Barrientos, A., del Cerro, J., Valero, C., 2022. Trend Technologies for Robotic
553 Fertilization Process in Row Crops. Front Robot AI 9.
554 https://doi.org/10.3389/frobt.2022.808484

555 Daszykowski, M., Walczak, B., Massart, D.L., 2002. Representative subset selection. Anal Chim Acta
556 468, 91–103. https://doi.org/10.1016/S0003-2670(02)00651-7

557 De Benedetto, D., Castrignanò, A., Rinaldi, M., Ruggieri, S., Santoro, F., Figorito, B., Gualano, S.,
558 Diacono, M., Tamborrino, R., 2013. An approach for delineating homogeneous zones by using
559 multi-sensor data. Geoderma 199, 117–127. https://doi.org/10.1016/j.geoderma.2012.08.028

560 Diacono, M., Rubino, P., Montemurro, F., 2013. Precision nitrogen management of wheat . A review.
561 Agron Sustain Dev 33, 219–241. https://doi.org/10.1007/s13593-012-0111-z

562 Ehlert, D., Schmerler, J., Voelker, U., 2004. Variable Rate Nitrogen Fertilisation of Winter Wheat
563 Based on a Crop Density Sensor. Precis Agric 5, 263–273.
564 https://doi.org/10.1023/B:PRAG.0000032765.29172.ec

565 Evangelou, E., Stamatiadis, S., Schepers, J.S., Glampedakis, A., Glampedakis, M., Dercas, N., Tsadilas,
566 C., Nikoli, T., 2020. Evaluation of sensor-based field-scale spatial application of granular N to
567 maize. Precis Agric 21, 1008–1026. https://doi.org/10.1007/s11119-019-09705-2

568 Ferreira, J.F., Portugal, D., Andrada, M.E., Machado, P., Rocha, R.P., Peixoto, P., 2023. Sensing and
569 Artificial Perception for Robots in Precision Forestry: A Survey. Robotics 12, 139.
570 https://doi.org/10.3390/robotics12050139

571 Finger, R., Swinton, S.M., El Benni, N., Walter, A., 2019. Precision Farming at the Nexus of
572 Agricultural Production and the Environment. https://doi.org/10.1146/annurev-resource-
573 100518

574 Gonzalez-de-Soto, M., Emmi, L., Garcia, I., Gonzalez-de-Santos, P., 2015. Reducing fuel consumption
575 in weed and pest control using robotic tractors. Comput Electron Agric 114, 96–113.
576 https://doi.org/10.1016/j.compag.2015.04.003

577 Guerrero, A., De Neve, S., Mouazen, A.M., 2021a. Current sensor technologies for in situ and on-line
578 measurement of soil nitrogen for variable rate fertilization: A review, in: Advances in
579 Agronomy. Academic Press, pp. 1–38. https://doi.org/10.1016/bs.agron.2021.02.001

Guerrero, A., De Neve, S., Mouazen, A.M., 2021b. Data fusion approach for map-based variable-rate nitrogen fertilization in barley and wheat. Soil Tillage Res 205. https://doi.org/10.1016/j.still.2020.104789

Hopkins, B.G., 2013. Russet burbank potato phosphorus fertilization with dicarboxylic acid copolymer additive. J Plant Nutr 36, 1287–1306. https://doi.org/10.1080/01904167.2013.785565

Iqbal, J., Xu, R., Halloran, H., Li, C., 2020. Development of a Multi-Purpose Autonomous Differential Drive Mobile Robot for Plant Phenotyping and Soil Sensing. Electronics (Basel) 9, 1550. https://doi.org/10.3390/electronics9091550

Javadi, S.H., Guerrero, A., Mouazen, A.M., 2022. Clustering and Smoothing Pipeline for Management Zone Delineation Using Proximal and Remote Sensing. Sensors 22, 645. https://doi.org/10.3390/S22020645

Kazlauskas, M., Šarauskis, E., Lekavičienė, K., Naujokienė, V., Romaneckas, K., Bručienė, I., Buragienė, S., Steponavičius, D., 2022. The Comparison Analysis of Uniform-and Variable-Rate Fertilizations on Winter Wheat Yield Parameters Using Site-Specific Seeding. Processes 10. https://doi.org/10.3390/PR10122717

King, A., 2017. Technology: The Future of Agriculture. Nature 544, S21–S23. https://doi.org/10.1038/544S21a

Kitić, G., Krklješ, D., Panić, M., Petes, C., Birgermajer, S., Crnojević, V., 2022. Agrobot Lala—An Autonomous Robotic System for Real-Time, In-Field Soil Sampling, and Analysis of Nitrates. Sensors 22, 4207. https://doi.org/10.3390/s22114207

Koch, B., Khosla, R., Frasier, W.M., Westfall, D.G., Inman, D., 2004. Economic Feasibility of Variable-Rate Nitrogen Application Utilizing Site-Specific Management Zones. Agron J 96, 1572–1580. https://doi.org/10.2134./agronj2004.1572

Koch, M., Naumann, M., Pawelzik, E., Gransee, A., Thiel, H., 2020. The Importance of Nutrient Management for Potato Production Part I: Plant Nutrition and Yield. Potato Res 63, 97–119. https://doi.org/10.1007/s11540-019-09431-2

Lu, Z., Wang, Y., Degryse, F., Huang, C., Hou, C., Wu, L., Jiang, R., Mclaughlin, M.J., Zhang, F., 2022. Magnesium-fortified phosphate fertilizers improve nutrient uptake and plant growth without reducing phosphorus availability. Pedosphere 32, 744–751. https://doi.org/10.1016/j.pedsph.2022.06.010

Maleki, M.R., Mouazen, A.M., De Ketelaere, B., Ramon, H., De Baerdemaeker, J., 2008. On-the-go variable-rate phosphorus fertilisation based on a visible and near-infrared soil sensor. Biosyst Eng 99, 35–46. https://doi.org/doi:10.1016/j.biosystemseng.2007.09.007

Mao, J., Niu, W., Wang, H., Zhang, B., Cao, Z., Guo, Z., Zhao, H., Zhou, C., Gong, X., 2020. A Agricultural Spraying and Fertilization Robot based on Visual Navigation, in: 15th IEEE Conference on Industrial Electronics and Applications (ICIEA). IEEE, pp. 586–591. https://doi.org/10.1109/ICIEA48937.2020.9248224

Montero, J.M., Fernández-Avilés, Gema., Mateu, Jorge., 2015. Spatial and spatio-temporal geostatistical modeling and kriging, 1st Edition. ed. John Wiley & Sons Ltd, West Sussex.

Mouazen, A.M., 2006. Soil Survey Device. International publication published under the patent cooperation treaty (PCT). World Intellectual Property Organization, International Bureau. International Publication Number: WO2006/015463; PCT/BE2005/000129; IPC: G01N21/00; G01N21/0.

Mouazen, A.M., Kuang, B., 2016. On-line visible and near infrared spectroscopy for in-field phosphorous management. Soil Tillage Res 155, 471–477. https://doi.org/10.1016/j.still.2015.04.003

Munnaf, M.A., Castillo, A.G., Mouazen, A.M., 2023. A novel approach to map-sensor-based site-specific nitrogen fertilisation in winter wheat, in: Precision Agriculture '23. Wageningen Academic Publishers, The Netherlands, pp. 299–306. https://doi.org/10.3920/978-90-8686-947-3_36

Munnaf, M.A., Haesaert, G., Mouazen, A.M., 2022. Site-Specific Seeding for Maize Production Using Management Zone Maps Delineated with Multi-sensors Data Fusion Scheme. Soil Tillage Res 220, 1-16]. https://doi.org/10.1016/j.still.2022.105377

Munnaf, Muhammad Abdul, Haesaert, G., Mouazen, A.M., 2020a. Map-based site-specific seeding of seed potato production by fusion of proximal and remote sensing data. Soil Tillage Res 206, 104801. https://doi.org/10.1016/j.still.2020.104801

Munnaf, M.A., Haesaert, G., Van Meirvenne, M., Mouazen, A.M., 2021. Multi-sensors data fusion approach for site-specific seeding of consumption and seed potato production. Precis Agric 22, 1890–1917. https://doi.org/10.1007/s11119-021-09817-8

Munnaf, M.A., Haesaert, G., Van Meirvenne, M., Mouazen, A.M., 2020. Site-specific seeding using multi-sensor and data fusion techniques: A review, in: Spark, D.L. (Ed.), Advances in Agronomy. Academic Press, Amsterdam, pp. 241–323. https://doi.org/10.1016/bs.agron.2019.08.001

Munnaf, Muhammad Abdul, Haesaert, G., Van Meirvenne, M., Mouazen, A.M., 2020b. Map-based site-specific seeding of consumption potato production using high-resolution soil and crop data fusion. Comput Electron Agric 178, 105752. https://doi.org/10.1016/j.compag.2020.105752

Munnaf, M.A., Mouazen, A.M., 2023. An automated system of soil sensor-based site-specific seeding for silage maize: A proof of concept. Comput Electron Agric 209, 107872. https://doi.org/10.1016/j.compag.2023.107872

Munnaf, M.A., Mouazen, A.M., 2021. Optimising site-specific potato seeding rates for maximum yield and profitability. Biosyst Eng 212, 126–140. https://doi.org/10.1016/j.biosystemseng.2021.10.006

Naumann, M., Koch, M., Thiel, H., Gransee, A., Pawelzik, E., 2020. The Importance of Nutrient Management for Potato Production Part II: Plant Nutrition and Tuber Quality. Potato Res. https://doi.org/10.1007/s11540-019-09430-3

Nawar, S., Corstanje, R., Halcro, G., Mulla, D., Mouazen, A.M., 2017. Delineation of Soil Management Zones for Variable-Rate Fertilization, in: Spark, D.L. (Ed.), Advances in Agronomy. Academic press, Ansterdam, pp. 175–245. https://doi.org/10.1016/bs.agron.2017.01.003

Ørum, J.E., Tamirat, T.W., Pedersen, S.M., Stratton, A.D.H., Veldhuisen, B., Hilbrands, H., 2023. Optimal use of agricultural robot in arable crop rotation: A case study from the Netherlands. Smart Agricultural Technology 5, 100261. https://doi.org/10.1016/j.atech.2023.100261

661 Roth, S., 2017. Partial Budgeting for Agricultural Business. Publications Distribution Center, The
662 Pennsylvania State University, Fourth 1–8.

663 Rousseeuw, P.J., 1987. Silhouettes: A graphical aid to the interpretation and validation of cluster
664 analysis. J Comput Appl Math 20, 53–65. https://doi.org/10.1016/0377-0427(87)90125-7

665 Savitzky, A., Golay, M.J.E., 1964. Smoothing and Differentiation of Data by Simplified Least Squares
666 Procedures. Anal Chem 36, 1627–1639. https://doi.org/10.1021/ac60214a047

667 Schillaci, C., Tadiello, T., Acutis, M., Perego, A., 2021. Reducing topdressing N fertilization with
668 variable rates does not reduce maize yield. Sustainability (Switzerland) 13.
669 https://doi.org/10.3390/SU13148059

670 Silva, J.G., França, M.G.C., Gomide, F.T.F., Magalhaes, J.R., 2013. Different Nitrogen Sources Affect
671 Biomass Partitioning and Quality of Potato Production in a Hydroponic System. American
672 Journal of Potato Research 90, 179–185. https://doi.org/10.1007/s12230-012-9297-5

673 Stamatiadis, S., Schepers, J.S., Evangelou, E., Glampedakis, A., Glampedakis, M., Dercas, N., Tsadilas,
674 C., Tserlikakis, N., Tsadila, E., 2020. Variable-rate application of high spatial resolution can
675 improve cotton N-use efficiency and profitability. Precis Agric 21, 695–712.
676 https://doi.org/10.1007/s11119-019-09690-6

677 Stamatiadis, S., Schepers, J.S., Evangelou, E., Tsadilas, C., Glampedakis, A., Glampedakis, M., Dercas,
678 N., Spyropoulos, N., Dalezios, N.R., Eskridge, K., 2018. Variable-rate nitrogen fertilization of
679 winter wheat under high spatial resolution. Precis Agric 19, 570–587.
680 https://doi.org/10.1007/s11119-017-9540-7

681 Van Vliet, J.A., Giller, K.E., 2017. Mineral Nutrition of Cocoa, in: Wageningen University and Research
682 Centre. pp. 185–270. https://doi.org/10.1016/bs.agron.2016.10.017

683 Virk, S.S., Fulton, J.P., Porter, W.M., Pate, G.L., 2020. Row-crop planter performance to support
684 variable-rate seeding of maize. Precis Agric 21, 603–619. https://doi.org/10.1007/s11119-019-
685 09685-3

686 Yang, Q., Du, X., Wang, Z., Meng, Z., Ma, Z., Zhang, Q., 2023. A review of core agricultural robot
687 technologies for crop productions. Comput Electron Agric 206, 107701.
688 https://doi.org/10.1016/j.compag.2023.107701

689 Zhang, J., Guerrero, A., Mouazen, A.M., 2022. Simulation of variable-rate manure application under
690 different application scenarios. Soil Tillage Res 221, 105416.
691 https://doi.org/10.1016/j.still.2022.105416

692 Zhang, J., Guerrero, A., Mouazen, A.M., 2021. Map-based variable-rate manure application in wheat
693 using a data fusion approach. Soil Tillage Res 207. https://doi.org/10.1016/J.STILL.2020.104846

694 Zhou, W., Han, G., Liu, M., Li, X., 2019. Effects of soil pH and texture on soil carbon and nitrogen in
695 soil profiles under different land uses in Mun River Basin, Northeast Thailand. PeerJ 7, e7880.
696 https://doi.org/10.7717/peerj.7880

697